

Article

Unraveling the Association between Metabolic Changes in Inter-Genus and Intra-Genus Bacteria to Mitigate Clubroot Disease of Chinese Cabbage

Lanfang Wei ^{1,†}, Jun Yang ^{1,2,†}, Waqar Ahmed ¹ , Xinying Xiong ¹, Qi Liu ¹, Qiong Huang ^{1,*} and Guanghai Ji ^{1,*}

¹ Key Laboratory of Agriculture Biodiversity for Plant Disease Management under the Ministry of Education, Yunnan Agricultural University, Kunming 650201, China; wlfang2000@aliyun.com (L.W.); yangjun@cxtc.edu.cn (J.Y.); ahmed.waqar1083@yahoo.com (W.A.); xxy704671710@163.com (X.X.); liuqi_ynnd@163.com (Q.L.)

² Academy of Science and Technology, Chuxiong Normal University, Chuxiong 675000, China

* Correspondence: huangqiong88hs@163.com (Q.H.); jghai001@163.com (G.J.)

† These authors have contributed equally to this work and share the first authorship.

Abstract: Clubroot disease caused by the obligate parasite *Plasmodiophora brassicae* is a serious threat to cabbage production worldwide. Current clubroot control primarily relies on a fungicide, but this has a negative impact on the environment and the use of a single biocontrol agent cannot efficiently control the disease. Thus, the combined application of different biocontrol agents has been proposed as a promising alternative. In this study, we used bacterial biocontrol agents as a co-culture (inter-genus and intra-genus) and mono-culture to mitigate the clubroot disease of Chinese cabbage. We evaluated their biocontrol effect and plant growth promoter (PGP) traits in in vitro and in vivo experiments. This study revealed that the inter-genus bacterial co-culture significantly suppresses the incidence of clubroot disease and enhances plant growth compared with intra-genus and mono-culture. In pairwise interaction, we observed that *Bacillus cereus* BT-23 promotes the growth of *Lysobacter antibioticus* 13-6 (inter-genus bacterial co-culture), whereas *L. capsici* ZST1-2 and *L. antibioticus* 13-6 (intra-genus microbial co-culture) are antagonists to each other. Furthermore, a total of 5575 metabolites, 732 differentially expressed metabolites (DEMs), and 510 unique metabolites were detected through the LC-MS/MS technique in the bacterial co-culture. The number of unique metabolites in inter-genus bacterial co-culture (393 metabolites) was significantly higher than in the intra-genus bacterial co-culture (117 metabolites). Further analysis of DEMs showed that the DEMs were mainly involved in four kinds of metabolism pathways, i.e., carbohydrate metabolism, amino acid metabolism, nucleotide metabolism, and metabolism of cofactors and vitamins. The contents of some secondary metabolites with biocontrol activity and plant growth-promoting functions were increased in inter-genus bacterial co-culture, indicating that inter-genus bacterial co-culture has a solid potential to suppress clubroot disease. We conclude that the inter-genus bacterial interaction changes the community metabolism and improves several secondary metabolites functions with respect to disease control and PGP ability.

Keywords: *Plasmodiophora brassicae*; biological control; disease incidence; bacterial co-culture; metabolomics analysis



Citation: Wei, L.; Yang, J.; Ahmed, W.; Xiong, X.; Liu, Q.; Huang, Q.; Ji, G. Unraveling the Association between Metabolic Changes in Inter-Genus and Intra-Genus Bacteria to Mitigate Clubroot Disease of Chinese Cabbage. *Agronomy* **2021**, *11*, 2424. <https://doi.org/10.3390/agronomy11122424>

Academic Editor:
Maryline Magnin-Robert

Received: 2 November 2021
Accepted: 26 November 2021
Published: 28 November 2021

Publisher's Note: MDPI stays neutral with regard to jurisdictional claims in published maps and institutional affiliations.



Copyright: © 2021 by the authors. Licensee MDPI, Basel, Switzerland. This article is an open access article distributed under the terms and conditions of the Creative Commons Attribution (CC BY) license (<https://creativecommons.org/licenses/by/4.0/>).

1. Introduction

Chinese cabbage (*Brassica rapa* L. ssp) is an economically important vegetable crop widely cultivated in China and worldwide. Clubroot disease caused by obligate biotrophic parasite *Plasmodiophora brassicae* is a serious threat to Chinese cabbage production and results in significant yield losses [1]. *P. brassicae* has prevailed in more than 60 countries and yield losses have been recorded up to 10–15% [2]. In China, clubroot disease is widely distributed in all cabbage-growing regions. However, the regions of Yunnan, Sichuan, and

Chongqing are badly affected by this disease and yield losses are reported to be between 20 and 30% [3]. The disease development is characterized by the formation of massive galls on the roots that block the uptake of water and essential nutrients from the soil [4]. Management of clubroot disease is a significant challenge because the pathogen is confined primarily to the host. Millions of resting spores are produced from infected roots that can survive in a dormant form in the soil for many years [5]. Therefore, finding strategies for the management of clubroot disease of Chinese cabbage is urgently needed.

Integrated disease management strategies, i.e., breeding resistant cultivars, fungicides, crop rotation, and biocontrol agents, have been adopted to control the clubroot disease of cruciferous crops [6–8]. Many studies have proven that *Lysobacter antibioticus* 13-6 exhibits a potent antagonist effect and significantly suppresses clubroot disease by producing antimicrobial substances, i.e., p-aminobenzoic acid [9,10]. Biocontrol agents (BCAs) may exert different mechanisms to suppress *P. brassicae* infection. The activity of individual BCAs against *P. brassicae* is relatively limited, which is a major constraint for commercial use [11]. Application of microbial co-culture (combination of BCAs) has been suggested as a practical approach with multiple beneficial traits to plants, i.e., disease suppression and plant growth promoter (PGP) [11,12].

Cai et al. 2021 [13] reported that soil physicochemical properties and the functional diversity of rhizospheric microorganisms play an important role in developing soilborne diseases. The biochar application significantly reduced the incidence of soilborne diseases by altering the soil physicochemical properties and reshaping the soil microbial diversity [14]. Fu et al. 2018 [15] reported that *L. antibioticus* 13-6 and *B. cereus* BT-23 efficiently control the clubroot disease of Chinese cabbage and act as a plant growth promoter. Zhang et al. 2020 [16] used *L. antibioticus* 13-6, *L. capsici* ZST1-2, and *B. cereus* BT-23 along with other BCAs as microbial consortia; results revealed that the application of microbial consortia significantly mitigates the incidence of *Fusarium* wilt of *Panax notoginseng*, acts as a PGP, and improves the ginsenoside contents.

Metabolomics provides a comprehensive depiction of a microbial community and provides insights into the mechanism involved in the metabolic process for metabolic crosstalk. To date, a number of researchers have used metabolomics approaches to unravel the antagonistic mechanism of microbial co-culture [17,18]. Metabolomics approach is used to study the ecological bacterial communication interactions by comparing the metabolites contents in co-culture and pure culture [19]. However, the interaction between inter-genus and intra-genus biocontrol agents that affect the production and functioning of metabolites is still unknown.

Here, we further extended the knowledge of metabolite-mediated functioning driven by bacterial inter-genus and intra-genus community interactions. In this study, we used the metabolomics approach to investigate the metabolite composition and pathways for bacterial co-culture composed of inter-genus (*L. antibioticus* 13-6 + *B. cereus* BT-23) and intra-genus (*L. antibioticus* 13-6 + *L. capsici* ZST1-2) bacteria. We hypothesized that this study provides new insight into the biocontrol mechanism of clubroot disease of Chinese cabbage through the application of inter-genus and intra-genus bacteria.

2. Materials and Methods

2.1. Experimental Site Description

The whole experiment was performed at Yunnan Agricultural University, Kunming (24.8801° N, 102.8329° E), China. In vitro experiments were performed in the Key Laboratory of Agriculture Biodiversity for Plant Disease Management and in vivo experiments were performed in a greenhouse under controlled conditions. The greenhouse conditions were maintained at 30 °C day and 20 °C night temperature with 10 h light and 14 h dark photoperiod.

2.2. Preparation of Pathogen Spore Suspension

The root galls were collected from a clubroot infected field in Hexi County, Yuxi City (24°20'49" N 102°31'37" E), Yunnan Province, China. Root galls were stored at 4 °C until use, then defrosted at room temperature (20 °C) and identified as pathotype 4 using the classification methodology of Liu et al. 2019 [1]. Briefly, 10 g of fresh gall roots were homogenized in (1:3, *w/v*) 30 mL sterilized distilled water (sdH₂O) in a mechanical blender and filtered through nylon cloth. Spore suspensions were cleaned by repeated (five times) centrifugation at 2000 rpm for 5 min. The spore pellets were collected in the precipitate and the final concentration of spores was adjusted to 5×10^7 spores/mL using a hemocytometer [1].

2.3. Bacterial Strains, Growth Medium, Culture Conditions, and Assembly of Bacterial Co-Culture and Mono-Culture

Bacterial strains with strong antagonistic activity used in this study were previously isolated and preserved in our laboratory. Three strains of biocontrol bacteria, one from genus *Bacillus*; *B. cereus* BT-23 (BC) and two from genus *Lysobacter*; *L. antibioticus* 13-6 (LA) and *L. capsici* ZST1-2 (LC), were selected as bacterial co-culture and single strain, as follows: (i) *L. antibioticus* 13-6, *L. capsici* ZST1-2, and *B. cereus* BT-23 as single-core strain, (ii) *L. antibioticus* 13-6 + *B. cereus* BT-23 as inter-genus bacterial co-culture, and (iii); *L. antibioticus* 13-6 + *L. capsici* ZST1-2 as intra-genus bacterial co-culture. Before the start of the experiment, each bacterial strain was cultured on a King's B (KB) medium plate (Peptone 20 g/L, KH₂PO₄ 1.5 g/L, MgSO₄·7H₂O 1.5 g/L, Glycerol 10 mL/L, Agar 20 g/L, and pH 7.0) at 28 °C for 48 h. A single colony was picked from each pure culture and transferred into 500 mL of KB broth incubated at 28 °C and 160 rpm for 24 h. The optical density of the culture medium was adjusted to an OD_{600nm} = 0.5 using a spectrophotometer (GE Uitrospec 2100 pro) [16]. A 250 mL culture medium was taken from one bacterial strain and mixed with another to assemble the bacterial co-culture.

2.4. In-Vivo Assay

2.4.1. Raising of Nursery

Seeds of Chinese cabbage cv. Luchunbai No.1 susceptible to clubroot were purchased from Qingdao International Seed Co., Ltd. (Shandong, China) and sown in floating foam polystyrene trays (162 wells) containing a mixture of nursery medium, i.e., sterilized soil, peat, vermiculite, and perlite (1:2:1:1, *v/v*, respectively), in a greenhouse according to the method of Li et al. 2010 [20] three weeks prior to use. The greenhouse temperature was maintained at 15 °C/ 30 °C (night and day) with 7–9 h day length using thermal insulation material.

2.4.2. Greenhouse Experiment

Greenhouse experiments were carried out at Yunnan Agricultural University, Kunming City, China, during the summer season in 2020. Three-week-old seedlings of Chinese cabbage variety Luchunbai No.1 were transplanted into pots (25 × 29 cm) containing 3 kg of double sterilized soil. To overcome the nutrient deficiency, fertilizer was mixed thoroughly in the soil before transplanting [20]. The experiment was carried out under six conditions: *L. antibioticus* 13-6 (T1), *L. capsici* ZST1-2 (T2), *B. cereus* BT-23 (T3), *L. antibioticus* 13-6 + *B. cereus* BT-23 (T4), *L. antibioticus* 13-6 + *L. capsici* ZST1-2 (T5), and control (CK; application of pathogen). One week after transplantation, each pot (30 mL/pot) was artificially inoculated via the root drenching method with 5×10^7 ·mL⁻¹ spore suspensions of *P. brassicae*. Bacterial co-culture and single strain were applied 20 mL/pot thrice after one, two, and three weeks of transplantation, whereas CK was treated with ddH₂O 20 mL/pot. The experiment was conducted under a completely randomized design with 45 plants (3 plants/pot) in each treatment (15 plants per replication) and each treatment was repeated thrice.

2.4.3. Evaluation of Plant Growth Promotion, Disease Index, and Biocontrol Efficacy

The effect of bacterial co-culture and single strain as plant growth promoter (PGP) and biocontrol were investigated after four weeks of transplantation. Plant growth promotion ability was determined in terms of fresh weight/plant (FW). The disease incidence was investigated using a six-point rating scale clubroot disease described by Liu et al. 2018 [21]. The disease incidence (Di) %, disease index (DI) %, and control efficacy (CE) % were calculated using the following formulas: $Di (\%) = (\text{Numbers of diseased plants} / \text{Total numbers of investigated plants}) \times 100$; $DI (\%) = [\sum (\text{Numbers of diseased plants} \times \text{Relative value}) / (\text{Total numbers of investigated plants} \times \text{Highest disease rating scale})] \times 100$; and $CE (\%) = [(\text{Disease index of control} - \text{Disease index of treatment}) / \text{Disease index of control}] \times 100$.

2.5. Investigation of Pairwise Interactions between Biocontrol Strains

To quantify the type (facilitative, neutral, and antagonistic) and direction of each pairwise interaction between biocontrol strains, we compared the growth of each strain in mono-culture and co-culture according to the methodology of Lopatkin et al. 2019 [22]. Briefly, *L. antibioticus* 13-6, *B. cereus* BT-23, and *L. capsici* ZST1-2 were grown overnight in R2A broth (Peptone 0.5 g/L, Casamino acids 0.5 g/L, Yeast extract 0.5 g/L, Dextrose 0.5 g/L, Soluble starch 0.5 g/L, Dipotassium phosphate 0.3 g/L, Magnesium sulfate 0.5 g/L, Sodium pyruvate 0.3 g/L, and pH 7.0) incubated at 160 rpm and 28 °C for 12 h. To initiate mono-culture, one mL of pure culture from each strain was taken and inoculated into 50 mL of R2A broth. The same volume of pure culture from each strain was transferred into two flasks containing 50 mL of R2A broth to start the co-culture to investigate the pairwise interaction (intra-genus and inter-genus) and incubated overnight at 160 rpm and 28 °C.

The optical density of mono-culture and co-culture was adjusted $OD_{600\text{nm}} = 0.5$, and serial dilutions (10^5 – 10^6) of bacterial suspensions were prepared. A 0.1 mL aliquot from each dilution was taken and spread on R2A agar medium plates incubated at 28 °C for 48 h. The colony count method (CFU/mL) was adopted based on their distinct colony morphologies (LA; red, LC; yellow, and BC; white) to quantify the growth of each strain. The mono-culture productivity (MP) and co-culture productivity (CP) for each strain are labeled as MP (LA), MP (BC), and MP (LC); and CP (LA), CP (BC), and CP (LC), respectively. The pairwise interaction between two species (take I and II as examples) was determined by comparing the sum of endpoints of mono-culture productivity of I as MP_I and mono-culture productivity of II as MP_{II} with the final productivity of two strains co-culture productivity as CP_{I+II} . Thus, we expected the two strains interaction to be facilitative if $CP_{I+II} > MP_I + MP_{II}$, antagonistic if $CP_{I+II} < MP_I + MP_{II}$, and neutral if $CP = MP_I + MP_{II}$.

2.6. Growth Kinetics of Candidate Bacterial Strains in Co-Culture Assay

Species-specific growth curves were produced from co-cultures by multiplying the $OD_{600\text{nm}}$ measurements (total proportional biomass) by relative abundance ratios, derived across log-phase sampling points described by Lopatkin et al. 2019 [22]. Growth curves of bacterial strains in mono-culture and co-culture in R2A broth were monitored spectrophotometrically at $D_{600\text{nm}}$ (total proportional biomass), using culture medium as a blank. All growth experiments were performed in triplicate and mean results were recorded; the significance of regression coefficients was assessed by *t*-test ($\alpha = 0.05$). Growth rates (μ) were calculated by linear regression of log-transformed OD value vs. time for the exponential growth phase using the following formula: $\mu = (\log_i - \log_j) / (t_i - t_j)$, where OD_i is the OD at time i (t_i) and OD_j is the OD at time j (t_j).

2.7. Metabolomics Analysis

2.7.1. Metabolites Extraction

Metabolites were extracted from each sample (co-culture and mono-culture) as previously described by Zhai et al. 2018 [23]. The samples from the five different fermentations (mono-cultures: *L. antibioticus* 13-6, *B. cereus* BT-23, and *L. capsici* ZST1-2; and co-cultures: *L.*

antibioticus 13-6 + *B. cereus* BT-23 and *L. antibioticus* 13-6 + *L. capsici* ZST1-2) were collected in an early stationary growth phase; centrifuged at 8000 rpm and 4 °C for 5 min. Cell pellets were collected and washed twice with ice-cold phosphate-buffered saline (PBS). Each sample (minimum two biological replication) was immediately quenched in liquid nitrogen and stored at −80 °C. One mL of a pre-cooled mixture of methanol and ultra-pure water (4:1, *v/v*) was added to the collected cell pellet and transferred to a 1.5 mL glass vial, followed by cold chloroform (400 mL), and resuspended by pipette. The samples were then treated ultrasonically for 3 min in an ice bath (500 W; 6 s On and 6 s Off). The lysate (0.8 mL) was transferred to a 1.5 mL centrifuge tube and internal standard (20 µL of 2-chloro-L-phenylalanine (0.3 mg/mL) pre-dissolved in methanol was added and centrifuged at 12,000 rpm and 4 °C for 10 min. The supernatant (150 µL) from each tube was collected using crystal syringes, filtered through 0.22 µm microfilters, transferred to LC vials, and stored at −80 °C until LC-MS analysis.

2.7.2. LC-MS Analysis

LC-MS analysis was performed using AB ExionLC Ultra-High-Performance Liquid Chromatography (UHPLC) coupled with an AB TripleTOF 6600 plus UHD and Accurate-Mass Spectrometer. Briefly, an aliquot of 2 µL from each sample was injected and separated on a Waters ACQUITY UPLC@HSS T3 C18 column (100 mm × 2.1 mm, 1.8 µm). The parameters of LC-MS analysis were as follows: mobile phase A was 0.1% formic acid in the water and mobile phase B was 0.1% formic acid in acetonitrile [22]. The solvent gradient was as follows: *t* = 0 min, 5% B; *t* = 4 min, 30% B; *t* = 8 min, 50% B; *t* = 10 min, 80% B; *t* = 14 min, 100% B; *t* = 15 min, 5% B. The flow rate was 0.35 mL/min and the column temperature was 45 °C. All the samples were kept at 4 °C during the analysis.

Electrospray mass spectrometric (ESI-MS) analysis was conducted in positive ion and negative ion modes using the methodology of Van den Eede et al. 2015 [24]. The parameters of mass spectrometry were as follows: ion source temperature, 550 °C (+) and 550 °C (−); ion spray voltage, 5500 V (+) and 4500 V (−); curtain gas of 35 PSI; declustering potential, 80 V (+) and −80 V (−); collision energy, 10 eV (+) and −10 eV (−); and interface heater temperature, 550 °C (+) and 550 °C (−). For IDA analysis, the range of *m/z* was set as 40–1000 and the collision energy was 30 eV and −30 eV for the positive and negative ion modes, respectively.

2.7.3. Data Processing

Raw data of LC-MS was analyzed by the Progenesis QI v2.3 software (Nonlinear Dynamics, Newcastle, UK) using the following parameters as described by Cui et al. 2020 [25]: precursor tolerance was set at 5 ppm, product fragment tolerance was set at 10 ppm, and retention time (RT) tolerance was set 0.02 min. Internal standard detection parameters were deselected for peak RT alignment; isotopic peaks were excluded for analysis, noise elimination level was set at 10.00, and the minimum intensity was set to 15 % of base peak intensity. An Excel file (Excel 2016, Microsoft, USA) was obtained with three-dimensional datasets including *m/z*, peak RT, and peak intensities, and RT-*m/z* pairs were used as the identifier for each ion. The resulting matrix was further reduced by removing any peaks with a missing value (ion intensity = 0) in more than 50 % of samples.

The resulting three-dimensional data, the peak number, sample name, and normalized peak area were analyzed via the SIMCA software package (version 14.0, Umetrics, Umea, Sweden) from Shanghai luming biological technology CO., Ltd. (Shanghai, China) (<http://www.lumingbio.com>). Principal component analysis (PCA) and orthogonal partial least-squares discriminant analysis (OPLS-DA) were conducted to visualize the differences and select the differentially altered metabolites among the groups. The OPLS-DA model was employed with the first principal component of VIP (variable importance in the projection) values larger than 1.0 combined with a two-tailed Student's *t*-test (*p*-value < 0.05) to identify differential metabolites. Multivariate analysis was undertaken using the MetaboAnalyst 4.0 program (<http://www.metaboanalyst.ca/MetaboAnalyst/>) including PCA, OPLS-DA

(used to identify differentiated metabolites between the co-culture groups and mono-culture groups) and unsupervised hierarchical cluster analysis.

2.8. Identification of Differential Metabolites

A combined univariate and multivariate analysis method was used to screen the differentially expressed metabolites (DEMs) [26]. Each metabolite with a VIP value > 1, p -value < 0.05 [23] for each of the co-culture to mono-culture comparisons: inter-genus (*L. antibioticus* 13-6 + *B. cereus* BT-23) co-culture compared with mono-culture (*L. antibioticus* 13-6 and *B. cereus* BT-23), and intra-genus (*L. antibioticus* 13-6 + *L. capsici* ZST1-2) co-culture compared with mono-culture (*L. antibioticus* 13-6 and *L. capsici* ZST1-2), and was nominated as DEMs in four separate biomarker collections. DEMs were identified by Progenesis QI v2.3 (Nonlinear Dynamics, Newcastle, UK) data processing software based on public databases such as the Human Metabolome Database (<http://www.hmdb.ca>); Lipidmaps v2.3 (<http://www.lipidmaps.org>) and METLIN database (<https://metlin.scripps.edu>). According to the metabolites qualitative results (score) to screen the identified metabolites, the screening standard was selected as 36 points; less than 36 was deemed inaccurate and deleted.

2.9. Pathway Enrichment Analysis

The list of DEMs from each comparison was separately submitted to the non-commercial databases and the KEGG database (<http://www.genome.jp/KEGG/pathway.html>) for conducting the pathway enrichment analysis of *Escherichia coli* K-12 MG1655. The significantly varied pathways were identified under the different conditions with a cut-off of p -value < 0.05.

2.10. Statistical Analysis

Data were statistically analyzed using analysis of variance in Microsoft Excel 2013 and SPSS 19.0 statistical software [27]. Heatmaps and Venn diagrams were generated using R scripts in R software (Version 2.15.3). Significant differences among treatments were determined according to Duncan's multiple range test and Student's t -test at $p < 0.05$. All figures were processed and analyzed using Adobe Illustrator CC 2019 (Adobe Systems Inc., San Francisco, CA, USA).

3. Results

3.1. Effect of Microbial Co-Culture and Mono-Culture on Plant Growth and Incidence of Clubroot Disease

After four weeks of transplantation, the potential of bacterial co-culture and mono-culture as a plant growth promoter (PGP) and biocontrol were assessed. Five plants/replication were randomly uprooted from each treatment to investigate the PGP and biocontrol efficacy of biocontrol agents (BCAs) as mono-culture and co-culture. This study revealed that inter-genus bacterial co-culture significantly controls the incidence of clubroot disease, having a control effect of 57.53% and maximum yield of 127.35 g/plant compared with intra-genus bacterial co-culture (Figure S1 and Table 1). However, when applied as individual BCAs, *L. capsici* ZST1-2 efficiently control the incidence of clubroot disease, having a control effect of 46.57% and yield of 118.70 g/plant compared with *L. antibioticus* 13-6 and *B. cereus* BT-23 (Figure S1 and Table 1).

Table 1. Efficiency of biocontrol agents as co-culture and mono-culture against clubroot disease and plant growth promotion.

Treatment	Disease Index (%)	Control Effect (%)	Average Fresh Weight (g)/Plant
<i>L. antibioticus</i> 13-6	42.22 ± 2.11bc	42.73 ± 1.63b	104.65 ± 2.52c
<i>L. capsici</i> ZST1-2	39.40 ± 4.55bc	46.56 ± 2.58b	118.70 ± 3.03b
<i>B. cereus</i> BT-23	61.62 ± 6.51ab	16.43 ± 2.93c	102.40 ± 3.11c
<i>L. antibioticus</i> 13-6 + <i>B. cereus</i> BT-23	31.31 ± 5.65c	57.53 ± 3.47a	127.35 ± 7.46a
<i>L. antibioticus</i> 13-6 + <i>L. capsici</i> ZST1-2	46.67 ± 4.43bc	36.71 ± 0.91b	117.65 ± 2.07b
CK	73.73 ± 4.12a	/	52.10 ± 2.73d

Note: Data is represented as the standard error of means (\pm SEM) of at least 15 plants. According to Duncan's multiple range test, different small letters within a column show the significant differences among treatments ($p < 0.05$).

3.2. Determining Pairwise Interactions between Bacterial Co-Culture

Strain densities (CFU/mL) explain the facilitative effect and antagonistic effect in pairwise interactions (Figure 1). This study showed that a facilitative interaction (co-culture cell density > mono-culture density) was found in inter-genus (*L. antibioticus* 13-6 + *B. cereus* BT-23) biocontrol agents (Figure 1A,B), whereas in the case of intra-genus (*L. antibioticus* 13-6 + *L. capsici* ZST1-2) biocontrol agents, an antagonistic relationship (co-culture cell density < mono-culture density) was found (Figure 1C,D). Analysis of pairwise interactions revealed that *B. cereus* BT-23 shows the facilitative effect on *L. antibioticus* 13-6 and *L. antibioticus* 13-6 shows an inhibitory effect toward the *B. cereus* BT-23 population densities in inter-genus microbial co-culture. In contrast, an antagonistic relationship was found between intra-genus (*L. antibioticus* 13-6 + *L. capsici* ZST1-2) microbial co-culture (Figure 1E).

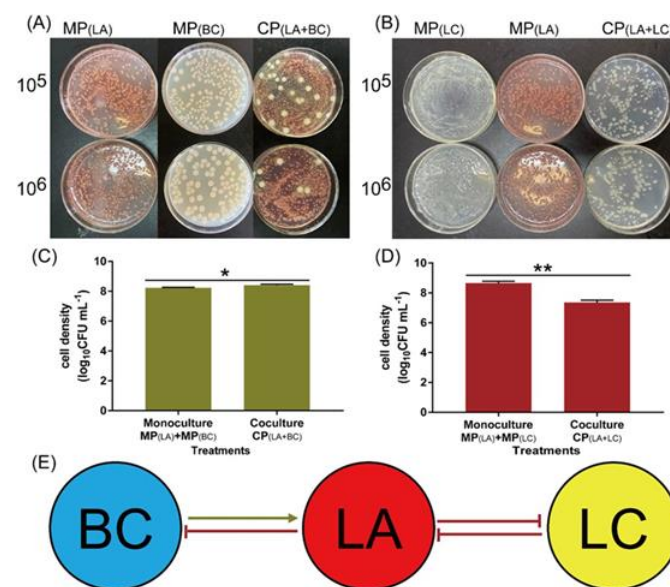


Figure 1. Determination of pairwise interactions between bacterial co-culture (inter-genus and intra-genus). Inter-genus co-culture assay (A), intra-genus co-culture assay (B), cell density of inter-genus co-culture assay (C), cell density of intra-genus co-culture assay (D), and network diagram showing the strength and directionality of pairwise interaction between different biocontrol agents (E). Significance differences among treatments is assessed according to Student's *t*-test at * $p < 0.05$ and ** $p < 0.001$.

3.3. Growth Rates of Mono-Culture and Co-Culture Biocontrol Agents

To explore the in-depth relationship between BCAs as single culture and co-culture (inter-genus and intra-genus), BCAs were grown on R₂A broth and their growth curves were recorded (Figure 2). Results of this study demonstrated that full growth curves of mono-cultures (*L. antibioticus* 13-6, *L. capsici* ZST1-2, and *B. cereus* BT-23) and co-cultures (inter-genus and intra-genus) reached the maximum population density after 36 h of incubation (Figure 2A). By comparing the growth rates of mono-culture, it was found that *L. capsici* ZST1-2 exhibited a higher growth rate ($\mu = 0.0407 \text{ h}^{-1}$), followed by *B. cereus* BT-23 (0.0344 h^{-1}) and *L. antibioticus* 13-6 (0.0311 h^{-1}) (Figure 2B–D). However, the growth rate of inter-genus BCAs (0.0420 h^{-1}) was significantly higher than intra-genus BCAs (0.0350 h^{-1}) and mono-culture BCAs (Figure 2E,F). These results confirmed a facilitative relationship between inter-genus BCAs strains *L. antibioticus* 13-6 and *B. cereus* BT-23, which promote cell density growth in a co-culture assay.

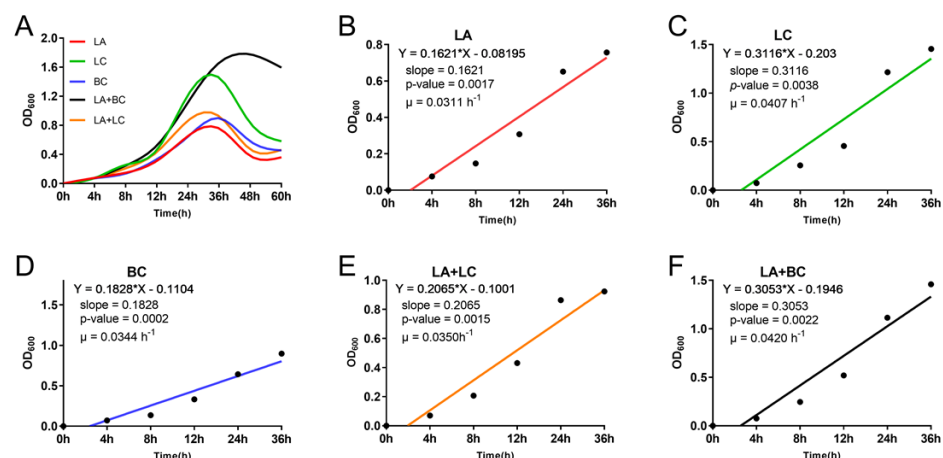


Figure 2. The growth dynamics of biocontrol agents (BCAs) when cultured as single strain and co-culture. (A) The full growth curves of BCAs as single strain and co-culture during the incubation. (B–F) The growth rates of each BCAs as single strain and co-culture.

3.4. Metabolomics Outline for Microbial Biocontrol Agents

Metabolites of mono-culture and co-culture BCAs were obtained using LC-MS through positive and negative ion modes. Representative base peak intensity (BPI) of chromatograms for mono-/co-cultures under both positive and negative ion modes are shown in Figure S2. A total of 3833 and 1742 metabolomics features (m/z) were obtained for the POS and NEG ion modes, respectively (Figure 3). We further explored the differences in the metabolic profiles of BCAs between co-culture and mono-culture. A total of 393 novel metabolites were detected in inter-genus bacterial co-culture (Figure 3A) and only 117 novel metabolites were detected in intra-genus bacterial co-culture (Figure 3B) through electrospray ionization of LC-MS (Table S1). The results revealed that inter-genus bacterial co-culture (*L. antibioticus* 13-6 + *B. cereus* BT-23) produced more novel metabolites than intra-genus bacterial co-culture (*L. antibioticus* 13-6 + *L. capsici* ZST1-2). A total of 5000 putative metabolites were detected through untargeted LC-MS analysis (Table S2). An unsupervised hierarchical clustering heatmap was generated based on fold changes (Figure 3C). Furthermore, PLS-DA analysis was adopted to explore the significant differences among a single strain and co-culture. The results of PLS-DA analysis of metabolome data harvested by LC-MS revealed that the inter-genus and intra-genus bacterial co-culture samples are different. Principal component analysis (PC-1 = 33.7%) and (PC-2 = 23.2%) accounted for the variance (Figure 3D). These results indicate that a significant difference was found in the metabolites of inter-genus and intra-genus bacterial co-culture. A multivariate analysis was conducted using a supervised technique to investigate how specific metabolites contributed between inter-genus and intra-genus co-culture BCAs.

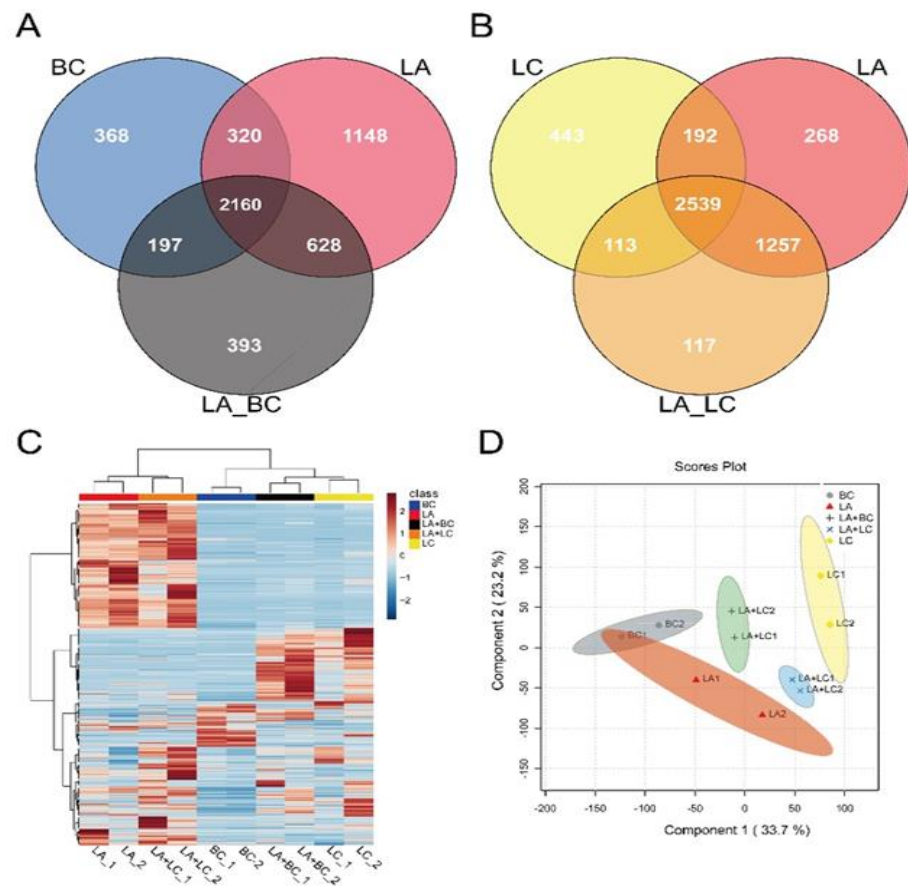


Figure 3. Metabolomics outline for the number of differently expressed metabolites of BCAs as single strain and co-culture. Inter-genus bacterial co-culture (A), intra-genus bacterial co-culture (B), unsupervised hierarchical cluster analysis carried out from untargeted metabolomics profiles of BCAs (C), principal component analysis (D).

3.5. Multivariate Analysis for Differentially Expressed Metabolites

Pairwise analysis of orthogonal projection to latent structures-discriminant analysis (OPLS-DA) of the metabolomics profiles was conducted to screen the differentially expressed metabolites (DEMs) ($VIP > 1$, $p < 0.05$) in inter-genus and intra-genus bacterial co-cultures (Figure 4). OPLS-DA model fitting parameters were tested 200 times by response permutation testing (RPT) with a goodness-of-fit $R^2Y = 1.0$ and goodness-of-prediction $Q^2Y = 1.0$. The variable important in projection (VIP) value for each metabolite was extracted from the OPLS-DA models, which indicates the importance of discriminating metabolites between co-culture and mono-culture BCAs.

For the screening of DEMs, a combined method of OPLS-DA and multivariate analysis was used. The significant DEMs between mono-culture and co-culture BCAs were selected using multivariate (OPLS-DA) and univariate analysis (Student's *t*-test). Each metabolite with a VIP value > 1 , p -value < 0.05 , and $|\log_2 \text{fold change}| > 1$ in each comparison were considered significantly changed metabolites (Table S3). After screening and identification of these metabolites, 260, 238, 60, and 174 metabolites were identified between inter-genus co-culture vs. *L. antibioticus* 13-6, inter-genus vs. *B. cereus* BT-23, intra-genus vs. *L. antibioticus* 13-6, and intra-genus vs. *L. capsici* ZST1-2, respectively (Table S4). These unique metabolites are mostly lipids and lipid-like molecules, organic acids and derivatives, benzenoids, nucleosides-nucleotides and analogues, organic oxygen compounds, organoheterocyclic compounds, and unclassified (Figure 5).

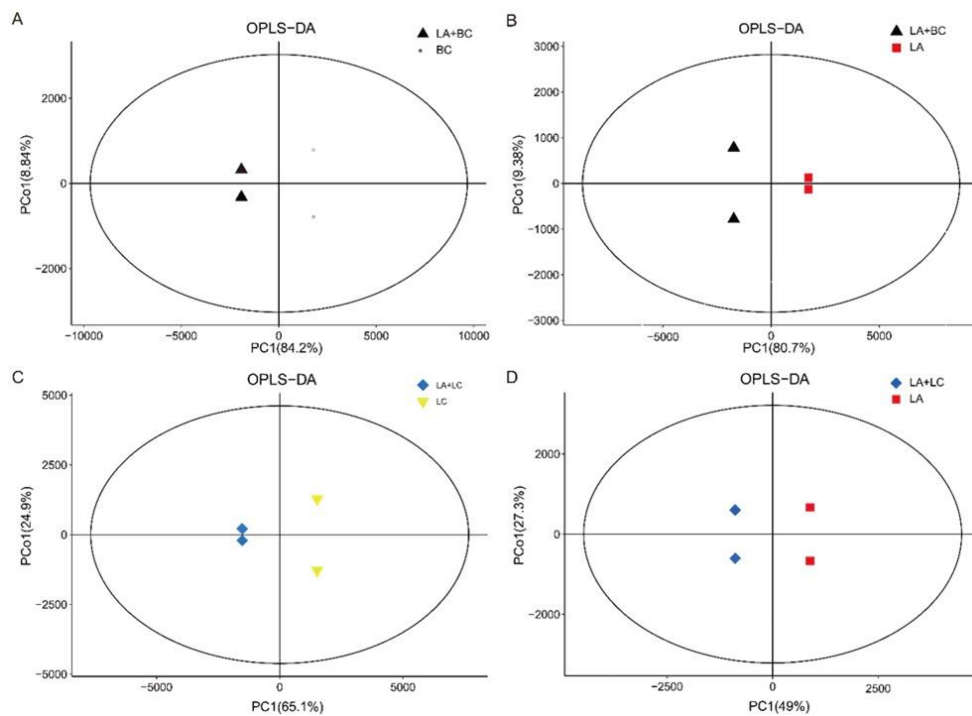


Figure 4. Orthogonal partial least-squares discrimination analysis (OPLS-DA) of different microbial culture metabolites. (A); *L. antibioticus* 13-6 and *B. cereus* BT-23 co-culture (LA+BC) vs. *B. cereus* BT-23 (BC). (B); *L. antibioticus* 13-6 and *B. cereus* BT-23 co-culture (LA+BC) vs. *L. antibioticus* 13-6 (LA). (C); *L. antibioticus* 13-6 and *L. capsici* ZST1-2 co-culture (LA+LC) vs. *L. capsici* ZST1-2 (LC). (D); *L. antibioticus* 13-6 and *L. capsici* ZST1-2 co-culture (LA+LC) vs. *L. antibioticus* 13-6 (LA).

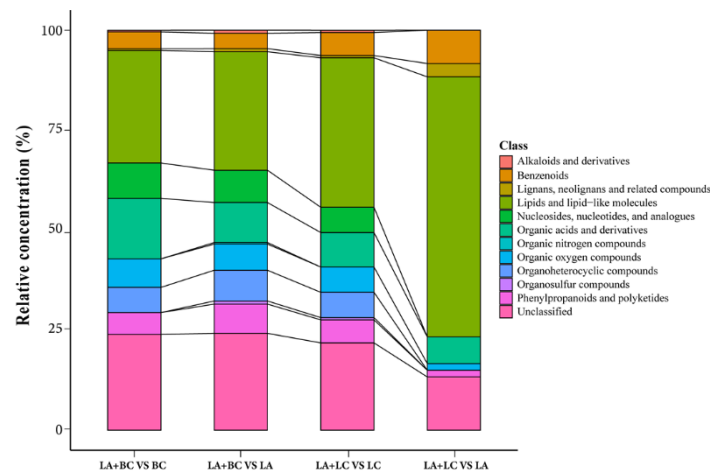


Figure 5. Analysis of differentially expressed metabolites between co-culture and mono-culture biocontrol agents. LA+BC vs. BC: *Lysobacter antibioticus* 13-6 and *Bacillus cereus* BT-23 co-culture vs. *B. cereus* BT-23; LA+BC vs. LA: *L. antibioticus* 13-6 and *B. cereus* BT-23 co-culture vs. *L. antibioticus* 13-6; LA+LC vs. LC: *L. antibioticus* 13-6 and *L. capsici* ZST1-2 co-culture vs. *L. capsici* ZST1-2; LA+LC vs. LA: *L. antibioticus* 13-6 and *L. capsici* ZST1-2 co-culture vs. *L. antibioticus* 13-6.

3.6. KEGG Enrichment Pathways for Differentially Expressed Metabolites

Pathway enrichment analysis was performed using the KEGG ID for DEMs to derive the metabolic enrichment pathway (Figure 6). We found a total of 17, 9, 11, and 2 enriched metabolic pathways between inter-genus co-culture vs. *B. cereus* BT-23 (Figure 6A), inter-genus co-culture vs. *L. antibioticus* 13-6 (Figure 6B), intra-genus co-culture vs. *L. capsici* ZST1-2 (Figure 6C), and intra-genus co-culture vs. *L. antibioticus* 13-6 (Figure 6D), respectively. The most relevant and significant metabolic pathways are carbohydrate,

amino, nucleotide, pyrimidine metabolism, amino sugar and nucleotide sugar metabolism, O-antigen nucleotide sugar biosynthesis, and purine metabolism.

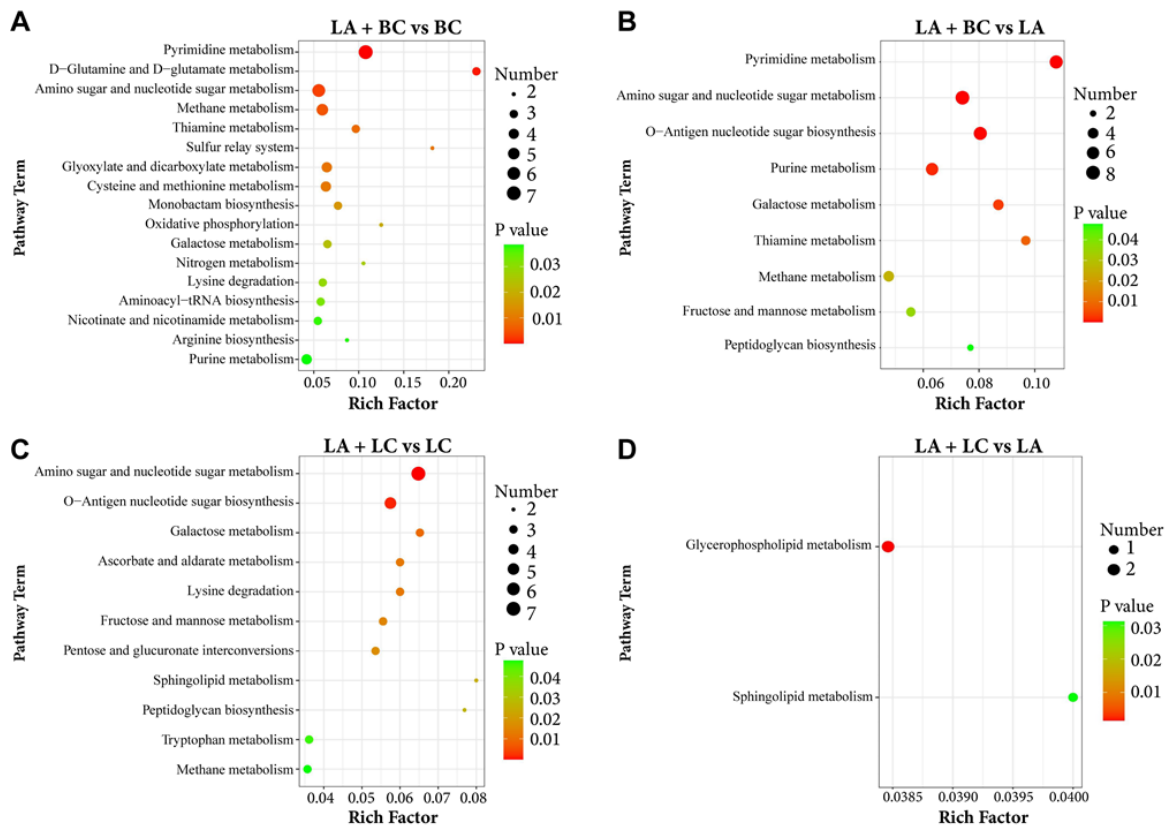


Figure 6. Analysis of KEGG enrichment pathway between different bacterial cultures $p < 0.05$. (A) *Lysobacter antibioticus* 13-6 and *Bacillus cereus* BT-23 co-culture (LA+BC) vs. *B. cereus* BT-23 (BC). (B) *L. antibioticus* 13-6 and *B. cereus* BT-23 co-culture (LA+BC) vs. *L. antibioticus* 13-6 (LA). (C) *L. antibioticus* 13-6 and *L. capsici* ZST1-2 co-culture (LA+LC) vs. *L. capsici* ZST1-2 (LC). (D) *L. antibioticus* 13-6 and *L. capsici* ZST1-2 co-culture (LA+LC) vs. *L. antibioticus* 13-6 (LA).

3.7. Interaction Network of Mono-Culture and Co-Culture Biocontrol Agents in Primary Metabolism Pathway

An interaction network was constructed for DEMs of inter-genus and intra-genus BCAs involved in the primary metabolism pathway (Figure 7). The DEMs between inter-genus bacterial co-culture vs. mono-culture and intra-genus bacterial co-culture vs. mono-culture were mainly involved in four primary metabolism pathways: carbohydrate metabolism, amino metabolism, nucleotide metabolism, and metabolism of cofactors and vitamins (Figure 8). In inter-genus bacterial co-culture vs. mono-culture, a total of 14, 13, 14, and 6 DEMs were detected in carbohydrate metabolism (12 up-regulated and two down-regulated), amino metabolism (six up-regulated and seven down-regulated), nucleotide metabolism (11 up-regulated and three down-regulated), and metabolism of cofactors and vitamins (four up-regulated and two down-regulated), respectively (Figure 8). In intra-genus bacterial co-culture vs. mono-culture, a total of 13, 5, 1, and 5 DEMs were detected in carbohydrate metabolism (three up-regulated and ten down-regulated), amino metabolism (two up-regulated and two down-regulated; whereas one DEM AHL showed both trends up- and down-regulated), nucleotide metabolism (one down-regulated), and metabolism of cofactors and vitamins (two up-regulated and three down-regulated), respectively. This result indicates that these metabolism pathways involved in energy metabolism in inter-genus and intra-genus BCAs were up-regulated and down-regulated, respectively.

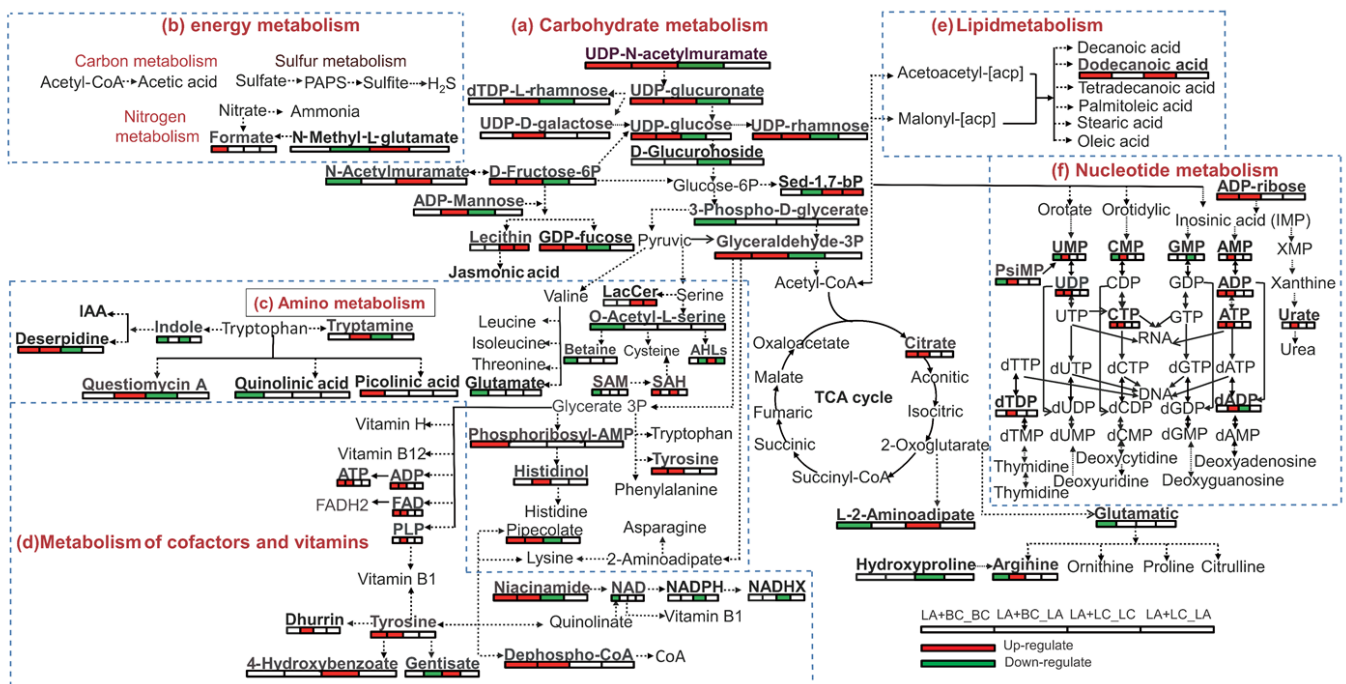


Figure 7. Visual analysis of metabolism network of carbohydrates, amino acids, fatty acids, nucleotides, cofactors-vitamins, and second productions in bacterial cultures. The data represent the expression of metabolites in the bacterial co-culture compared with the single strain. Note: red indicates up-regulation, green indicates down-regulation, and blank indicates no significant differences.

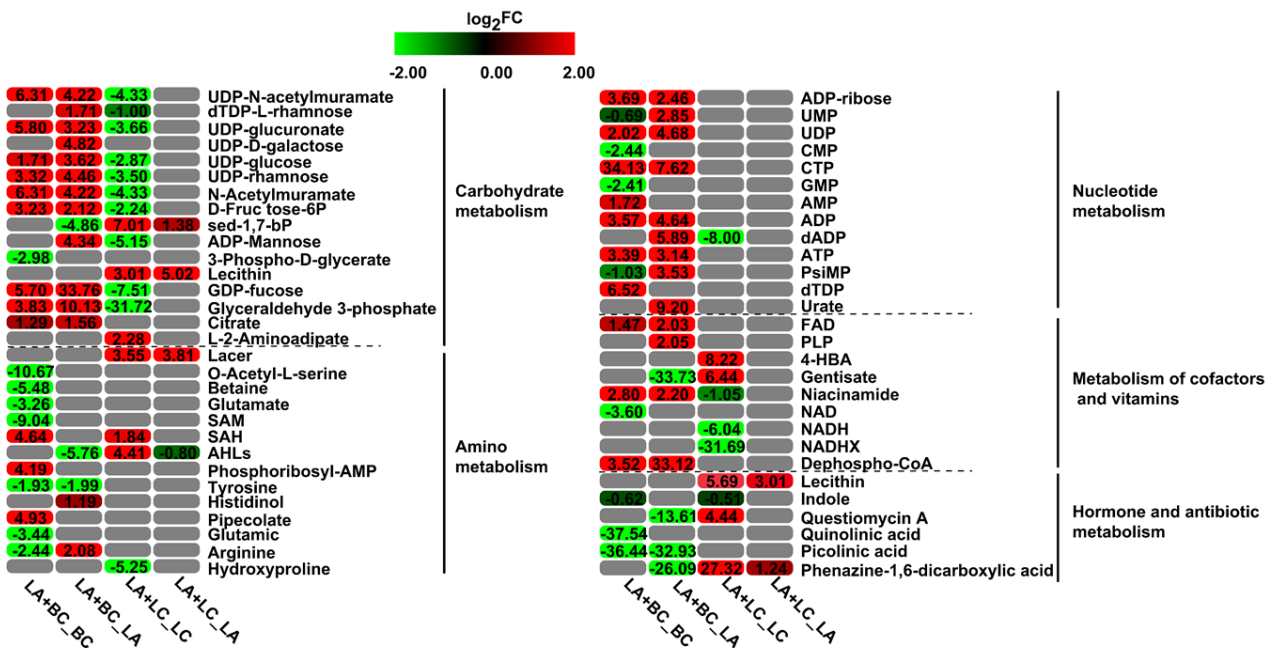


Figure 8. Quantification of differentially expressed metabolites involved in four primary metabolism and PGP-related pathways.

3.8. Differentially Expressed Metabolites Related to Plant Growth and Antimicrobial Function

The DEMs related to plant growth and antimicrobial activity between bacterial co-culture and mono-culture were involved in hormones and antibiotics metabolism (Figure 8). The two plant hormones, indole-3-lactic acid (IAA) and jasmonic acid (JA), were not directly detected in this study, but indole and lecithin are precursors for IAA and JA synthesis, and were detected by LC-MS, respectively. Indole was decreased in bacterial co-culture, but lecithin was increased in intra-genus bacterial co-culture. In addition, a significant

difference was found in four DEMs (Phenazine-1,6-dicarboxylic acid, Questioniomycin A, Quinolinic acid, and Picolinic acid) between inter-genus and intra-genus bacterial co-culture. These four DEMs were decreased in the inter-genus co-culture, but Questioniomycin A was increased in intra-genus bacterial co-culture (Figure 8 and Table S5).

4. Discussion

Clubroot disease caused by *P. brassicae* is a devastating soilborne disease of Chinese cabbage in China, especially in Yunnan, Sichuan, and Chongqing. The average yield losses are estimated to be 20–30%, but in a severe outbreak it causes an 80% yield reduction [1,3]. The pathogen persists in the soil for a long period and it is difficult to control the disease [21]. Many integrated disease management (IDM) strategies have been adopted, i.e., chemical control, cultural practices, and resistance variety, but have not yielded successful results. Biological control through disease suppressive BCAs such as *Bacillus* spp. and *Lysobacter* spp. plays an important role in controlling the clubroot disease [28]. The use of BCAs as microbial consortia due to their dual properties, i.e., antagonist and PGP, is considered an efficient method to control the incidence of soilborne diseases such as Fusarium wilt, clubroot, and bacterial wilt [12,16].

In this study, we used biocontrol agents (BCAs) (*Lysobacter antibioticus* 13-6, *Bacillus cereus* BT-23, and *L. capsici* ZST1-2) as co-culture (inter-genus and intra-genus) and mono-culture (single strain) to control the clubroot disease of Chinese cabbage and act as a PGP. This study revealed that *L. capsici* ZST1-2 significantly reduced the incidence of clubroot disease and enhanced plant growth compared with other single strain BCAs. However, the application of inter-genus bacteria (*L. antibioticus* 13-6 + *B. cereus* BT-23) has a superior effect as a biocontrol and plant growth promoter (PGP) compared with intra-genus (*L. antibioticus* 13-6 + *L. capsici* ZST1-2) and mono-culture bacteria. The reason for this is that, in an inter-genus bacterial co-culture, a facilitative association was present between *L. antibioticus* 13-6 and *B. cereus* BT-23. In contrast, in intra-genus bacterial co-culture, an antagonistic relationship was observed between *L. antibioticus* 13-6 and *L. capsici* ZST1-2.

The results of in vitro co-culture assay proved that facilitative interaction was found in inter-genus (*L. antibioticus* 13-6 + *B. cereus* BT-23) bacterial co-culture, whereas *L. capsici* ZST1-2 was found to be an antagonist to *L. antibioticus* 13-6 in intra-genus bacterial co-culture. Our results are similar to the findings of Sarma et al. 2015 [29] and Palmieri et al. 2017 [11], which proved that compatible microbes do not have an antagonist effect on each other when co-cultured in vitro and have an enhanced impact on plant growth promotion when applied as consortia/co-culture. The use of different species of microbes in microbial consortia further enhances biocontrol efficacies because different microbes occupy different niches in the rhizosphere and thereby restrict competition among them.

The advancements in metabolomics enabled us to track the changes in host metabolites in response to biotic and abiotic stress [30,31]. Previous studies provided limited knowledge on the metabolites and their systematic interaction modes, and were mainly focused on the growth factors induced by one strain [32]. In this study, we compared the untargeted metabolomics profiles of the inter-genus and intra-genus BCAs as co-culture and mono-cultures. A total of 732 DEMs were detected in this study through LC-MS analysis, and metabolic regulation was found to be different between co-culture and mono-culture BCAs. Inter-genus bacterial BCAs produced more novel metabolites than intra-genus bacterial BCAs. Furthermore, KEGG pathway enrichment analysis for DEMs showed that these DEMs were involved in carbon metabolism, nucleotide, amino acids metabolisms, cofactors (vitamins) metabolism, and secondary metabolism pathways. These pathways are responsible for the colonization, survival, and production of antibacterial compounds, and our results are similar to those of the previous studies [33,34].

The DEMs were significantly up-regulated in carbohydrate metabolism, amino acid metabolism, and nucleic acid metabolism in inter-genus BCAs compared with intra-genus BCAs. It was observed that the contents of tyrosine significantly increased in inter-genus bacterial co-culture compared with mono-culture. Many studies have proven that tyrosine

not only affects the synthesis of cofactors (e.g., NAD, NADP, and FAD) but also influences the production of vitamins (vitamin B1, vitamin B12, and vitamin H) [35,36]. Microbes in a microbial consortia compete for niche exclusion, nutrient acquisition, and cell-to-cell communication via metabolites [37]. The metabolic interactions through the exchange of small molecules help microbes to maintain their diversity and stability [38]. It was proven that when *B. megaterium* and *K. vulgare* are grown as co-culture, the metabolites contents were significantly higher than in *K. vulgare*, but no difference was found compared with *B. megaterium*; this may be because the metabolites produced by *B. megaterium* promote the growth of *K. vulgare* [39].

In this study, we found that some DEMs contents (involved in carbon metabolism, nucleotide, amino acids metabolism, and cofactors-vitamins metabolism pathways) were significantly higher in inter-genus co-culture + *L. antibioticus* 13-6, but were lower in inter-genus co-culture + *B. cereus* BT-23, e.g., Deoxythymidine diphosphate-l-rhamnose (dTDP-L-rhamnose), UDP-D-galactose, 3-Phospho-D-glycerate, Pyridoxal Phosphate (PLP), UMP, CMP, and arginine. It is speculated that the metabolites produced by *B. cereus* BT-23 promote the growth of *L. antibioticus* 13-6. We further verified the results of metabolomics analysis through colony growth in plate culture assay. The results revealed that *B. cereus* BT-23 promotes the growth of *L. antibioticus* 13-6, but the DEMs produced by *L. antibioticus* 13-6 to be used by *B. cereus* BT-23 were not detected. Further study is required on molecular biological techniques to construct an auxotrophic mutant strain of *B. cereus* BT-23 for co-culture assay with *L. antibioticus* 13-6.

Different metabolites produced by beneficial bacteria have been described as having a key function in the biological control of plant diseases [40,41]. Studies have proven that inter-genus microbial co-culture produced different DEMs than mono-culture, such as VOCs [42] and hormones [43]. The hormone IAA is involved in gall formation during the late infection stage [44], and SA- and JA-triggered defenses result in resistance after *P. brassicae* inoculation [45]. However, we did not directly detect these plant hormones as DEMs between microbial mono-culture and co-culture. Only indole and lecithin, as the precursors of IAA and JA synthesis, respectively, were identified. Indole was down-regulated in both microbial co-culture (inter-genus and intra-genus) and lecithin was up-regulated in intra-genus co-culture and mono-culture. However, this result does not prove that the co-culture products IAA and JA affect the Chinese cabbage resistance to *P. brassicae*.

Phenazine compounds produced by *L. antibioticus* have shown broad-spectrum antagonistic activity against many fungal and bacterial pathogens [46]. The contents of phenazine-1,6-dicarboxylic acid (PDC) were detected in high concentration in *L. antibioticus* 13-6 mono-culture but were not detected in the mono-culture of *B. cereus* BT-23 and *L. capsici* ZST1-2. However, the contents of PDC were decreased in inter-genus co-culture and maintained at a high level in intra-genus co-culture. These results show that PDC produced from *L. antibioticus* 13-6 is not affected by inter-genus and intra-genus BCAs. Some compounds, such as p-aminobenzoic acid (PABA) and 4-Hydroxyphenylacetic acid (4-HPA), are benzoic acid derivatives with strong antifungal activity [10]. The contents of 4-Hydroxybenzoic acid (4-HBA) and 4-HPA are regulated by tyrosine [47]. Our study found that tyrosine content significantly increased in inter-genus bacterial co-culture, whereas 4-HPA was not detected. Further study will be required to confirm the biocontrol potential of phenazine compounds against clubroot disease.

5. Conclusions

In this study, we combined the growth phenotypes and metabolomics status to explore the effect of intra-genus and inter-genus bacterial biocontrol agents (BCAs) as mono-culture and co-culture on the production and functioning of metabolites. It was concluded that the inter-genus bacterial co-culture (*L. antibioticus* 13-6 + *B. cereus* BT-23) significantly mitigated the clubroot disease of Chinese cabbage with PGP traits and produced a higher number of metabolites than intra-genus and mono-culture bacterial BCAs. Growth phenotypes

of inter-genus bacterial co-culture revealed that *B. cereus* BT-23 promotes the growth of *L. antibioticus* 13-6. The metabolomics profiling of the inter-genus bacterial co-culture exhibited global metabolite variations in carbon metabolism, nucleotide, amino acids metabolism, cofactors-vitamins metabolism, and secondary metabolites. The results clearly showed that the bacterial interactions between genera affect the production and type of metabolites. Some secondary metabolites that mediated functioning in disease suppression (biocontrol activity) increased significantly in the inter-genus co-culture. The increase in the content of secondary metabolites plays an important role in the biocontrol of the clubroot disease of Chinese cabbage. The presented co-culture growth phenotypes and metabolomics pathway will help researchers in the construction of microbial consortia. From an applied perspective, our study suggests that secondary metabolite-mediated functions can improve multiple ecosystem functions, including disease suppression and plant growth.

Supplementary Materials: The following are available online at <https://www.mdpi.com/article/10.3390/agronomy11122424/s1>. Figure S1; Effect of biocontrol agents (single and microbial consortia) as PGP and biocontrol against clubroot disease of Chinese cabbage (Age of plants: four weeks). *Lysobacter antibioticus* 13-6 (T1), *L. capsici* ZST1-2 (T2), *Bacillus cereus* BT-23 (T3), *L. antibioticus* 13-6 + *B. cereus* BT-23 (T4), *L. antibioticus* 13-6 + *L. capsici* ZST1-2 (T5), and control (CK; application of pathogen), Figure S2; Base peak chromatograms obtained from the LC-MS analysis of metabolites obtained from bacterial cultures. (A–E) represents the negative ion modes and (F–J) represents the positive ion modes of different bacterial cultures, respectively, Table S1, Novel metabolites in inter-genus and intra-genus biocontrol agents; Table S2, Untargeted LC-MS analysis for putative metabolites, Table S3, Multivariate analysis for DEMs; Table S4, Differentially expressed metabolites in inter-genus and intra-genus bacterial co-culture vs. mono-culture; Table S5, Expression of differentially expressed metabolites in inter-genus and intra-genus bacterial co-culture vs. mono-culture.

Author Contributions: Conceptualization, G.J. and L.W.; methodology, X.X., Q.L. and Q.H.; software, J.Y. and W.A.; formal analysis, L.W., J.Y. and W.A.; investigation, L.W., X.X. and Q.L.; resources, G.J.; data curation, L.W. and X.X.; writing—original draft preparation, L.W., J.Y. and W.A.; writing—review and editing, J.Y., W.A. and G.J.; supervision, L.W. and G.J.; project administration, G.J.; funding acquisition, G.J. and J.Y. All authors have read and agreed to the published version of the manuscript.

Funding: This study was financially supported by the National Key Research and Development Program of China (2019YFD1002000), the National Natural Science Foundation of China (No. 32060601), the Yunnan Ten Thousand Talents Plan Leading Talents of Industrial Technology Project of China (YNWR-CYJS-2019-046), and PhD research Startup Foundation of Chuxiong Normal University, China (BSQD2105).

Data Availability Statement: All supporting data is available online along with this manuscript as supplementary material.

Conflicts of Interest: The authors declare have no conflict of interest.

References

1. Liu, C.; Yang, Z.; He, P.; Munir, S.; He, P.; Wu, Y.; Ho, H.; He, Y. Fluazinam positively affected the microbial communities in clubroot cabbage rhizosphere. *Sci. Hortic.* **2019**, *256*, 108519. [[CrossRef](#)]
2. Wang, Y.; Luo, W.; Huang, Y.; Xu, L.; Yin, Y. Improved control of clubroot (*Plasmodiophora brassicae*) by a mixture of a fungicide and a plant defense inducer. *J. Plant Dis. Prot.* **2017**, *124*, 67. [[CrossRef](#)]
3. Chai, A.L.; Xie, X.W.; Shi, Y.X.; Li, B.J. Research status of clubroot (*Plasmodiophora brassicae*) on cruciferous crops in China. *Can. J. Plant Pathol.* **2014**, *36*, 142. [[CrossRef](#)]
4. Niemann, J.; Kaczmarek, J.; Książczyk, T.; Wojciechowski, A.; Jedryczka, M. Chinese cabbage (*Brassica rapa* ssp. *pekinensis*)—A valuable source of resistance to clubroot (*Plasmodiophora brassicae*). *Eur. J. Plant Pathol.* **2017**, *147*, 181. [[CrossRef](#)]
5. Zahr, K.; Sarkes, A.; Yang, Y.; Ahmed, H.; Zhou, Q.; Feindel, D.; Harding, M.W.; Feng, J. *Plasmodiophora brassicae* in Its Environment—: Effects of Temperature and Light on Resting Spore Survival in Soil. *Phytopathology* **2021**, *9*, 819524. [[CrossRef](#)] [[PubMed](#)]
6. Peng, L.; Zhou, L.; Li, Q.; Wei, D.; Ren, X.; Song, H.; Mei, J.; Si, J.; Qian, W. Identification of Quantitative Trait Loci for Clubroot Resistance in *Brassica oleracea* With the Use of *Brassica* SNP Microarray. *Front. Plant Sci.* **2018**, *9*, 822. [[CrossRef](#)] [[PubMed](#)]

7. Shah, N.; Sun, J.; Yu, S.; Yang, Z.; Wang, Z.; Huang, F.; Dun, B.; Gong, J.; Liu, Y.; Li, Y.; et al. Genetic variation analysis of field isolates of clubroot and their responses to Brassica napus lines containing resistant genes CRb and PbBa8. 1 and their combination in homozygous and heterozygous state. *Mol. Breed.* **2019**, *39*, 1–1153. [[CrossRef](#)]
8. Zhu, M.; He, Y.; Li, Y.; Ren, T.; Liu, H.; Huang, J.; Jiang, D.; Hsiang, T.; Zheng, L. Two New Biocontrol Agents Against Clubroot Caused by Plasmodiophora brassicae. *Front. Microbiol.* **2020**, *10*, 3099. [[CrossRef](#)] [[PubMed](#)]
9. Zhou, L.; Zhang, L.; He, Y.; Liu, F.; Li, M.; Wang, Z.; Ji, G. Isolation and characterization of bacterial isolates for biological control of clubroot on Chinese cabbage. *Eur. J. Plant Pathol.* **2014**, *140*, 159. [[CrossRef](#)]
10. Laborda, P.; Zhao, Y.; Ling, J.; Hou, R.; Liu, F. Production of Antifungal p-Aminobenzoic Acid in Lysobacter antibioticus OH13. *J. Agric. Food Chem.* **2018**, *66*, 630. [[CrossRef](#)]
11. Palmieri, D.; Vitullo, D.; De Curtis, F.; Lima, G. A microbial consortium in the rhizosphere as a new biocontrol approach against fusarium decline of chickpea. *Plant Soil* **2017**, *412*, 425. [[CrossRef](#)]
12. Goh, Y.K.; Marzuki, N.F.; Tuan Pa, T.N.F.T.; Goh, T.-K.; Kee, Z.S.; Goh, Y.K.; Yusof, M.T.; Vujanovic, V.; Goh, K.J. Biocontrol and Plant-Growth-Promoting Traits of Talaromyces apiculatus and Clonostachys rosea Consortium against Ganoderma Basal Stem Rot Disease of Oil Palm. *Microorganisms* **2020**, *8*, 1138. [[CrossRef](#)]
13. Cai, Q.; Zhou, G.; Ahmed, W.; Cao, Y.; Zhao, M.; Li, Z.; Zhao, Z. Study on the relationship between bacterial wilt and rhizo-spheric microbial diversity of flue-cured tobacco cultivars. *Eur. J. Plant Pathol.* **2021**, *160*, 265–276. [[CrossRef](#)]
14. Li, C.; Ahmed, W.; Li, D.; Yu, L.; Xu, L.; Xu, T.; Zhao, Z. Biochar suppresses bacterial wilt disease of flue-cured tobacco by improving soil health and functional diversity of rhizosphere microorganisms. *Appl. Soil Ecol.* **2021**, *171*, p104314. [[CrossRef](#)]
15. Fu, L.; Li, H.; Wei, L.; Yang, J.; Liu, Q.; Wang, Y.; Wang, X.; Ji, G. Antifungal and Biocontrol Evaluation of Four Lysobacter Strains Against Clubroot Disease. *Indian J. Microbiol.* **2018**, *58*, 353. [[CrossRef](#)]
16. Zhang, J.; Wei, L.; Yang, J.; Ahmed, W.; Wang, Y.; Fu, L.; Ji, G. Probiotic Consortia: Reshaping the Rhizospheric Microbiome and Its Role in Suppressing Root-Rot Disease of Panax notoginseng. *Front. Microbiol.* **2020**, *11*, 701. [[CrossRef](#)]
17. Ma, Q.; Bi, Y.-H.; Wang, E.-X.; Zhai, B.-B.; Dong, X.-T.; Qiao, B.; Ding, M.-Z.; Yuan, Y.-J. Integrated proteomic and metabolomic analysis of a reconstructed three-species microbial consortium for one-step fermentation of 2-keto-l-gulonic acid, the precursor of vitamin C. *J. Ind. Microbiol. Biotechnol.* **2019**, *46*, 21. [[CrossRef](#)]
18. Yao, Z.; Guo, Z.; Wang, Y.; Li, W.; Fu, Y.; Lin, Y.; Lin, W.; Lin, X. Integrated Succinylome and Metabolome Profiling Reveals Crucial Role of S-Ribosylhomocysteine Lyase in Quorum Sensing and Metabolism of Aeromonas hydrophila*. *Mol. Cell. Proteom.* **2019**, *18*, 200. [[CrossRef](#)] [[PubMed](#)]
19. Paul, C.; Mausz, M.A.; Pohnert, G. A co-culturing/metabolomics approach to investigate chemically mediated interactions of planktonic organisms reveals influence of bacteria on diatom metabolism. *Metabolomics* **2013**, *9*, 349. [[CrossRef](#)]
20. Li, J.; Zhao, X.; Nishimura, Y.; Fukumoto, Y. Correlation between Bolting and Physiological Properties in Chinese Cabbage (Brassica rapa L. pekinensis Group). *J. Jpn. Soc. Hortic. Sci.* **2010**, *79*, 294. [[CrossRef](#)]
21. Liu, C.; Yang, Z.; He, P.; Munir, S.; Wu, Y.; Ho, H.; He, Y. Deciphering the bacterial and fungal communities in clubroot-affected cabbage rhizosphere treated with Bacillus Subtilis XF-1. *Agric. Ecosyst. Environ.* **2018**, *256*, 12. [[CrossRef](#)]
22. Lopatkin, A.J.; Stokes, J.M.; Zheng, E.J.; Yang, J.H.; Takahashi, M.K.; You, L.; Collins, J.J. Bacterial metabolic state more accurately predicts antibiotic lethality than growth rate. *Nat. Microbiol.* **2019**, *4*, 2109. [[CrossRef](#)] [[PubMed](#)]
23. Zhai, Q.; Xiao, Y.; Narbad, A.; Chen, W. Comparative metabolomic analysis reveals global cadmium stress response of Lactobacillus plantarum strains. *Metallomics* **2018**, *10*, 1065. [[CrossRef](#)] [[PubMed](#)]
24. Van den Eede, N.V.D.; Cuykx, M.; Rodrigues, R.M.; Laukens, K.; Neels, H.; Covaci, A.; Vanhaecke, T. Metabolomics analysis of the toxicity pathways of triphenyl phosphite in HepaRG cells and comparison to oxidative stress mechanisms caused by aceta-minophen. *Toxicol. Vitro.* **2015**, *29*, 2045. [[CrossRef](#)] [[PubMed](#)]
25. Cui, H.; Li, Y.; Cao, M.; Liao, J.; Liu, X.; Miao, J.; Fu, H.; Song, R.; Wen, W.; Zhang, Z.; et al. Untargeted Metabolomic Analysis of the Effects and Mechanism of Nuciferine Treatment on Rats With Nonalcoholic Fatty Liver Disease. *Front. Pharmacol.* **2020**, *11*, 858. [[CrossRef](#)]
26. Booth, S.C.; Weljie, A.M.; Turner, R.J. Metabolomics reveals differences of metal toxicity in cultures of Pseudomonas pseudoalcaligenes KF707 grown on different carbon sources. *Front. Microbiol.* **2015**, *6*, 827. [[CrossRef](#)] [[PubMed](#)]
27. Wan, X.; Yang, J.; Ahmed, W.; Liu, Q.; Wang, Y.; Wei, L.; Ji, G. Functional analysis of pde gene and its role in the pathogenesis of Xanthomonas oryzae pv. oryzicola. *Infect. Genet. Evol.* **2021**, *94*, p105008. [[CrossRef](#)]
28. Ahmed, A.; Munir, S.; He, P.; Li, Y.; He, P.; Yixin, W.; He, Y. Biocontrol arsenals of bacterial endophyte: An imminent triumph against clubroot disease. *Microbiol. Res.* **2020**, *241*, 126565. [[CrossRef](#)]
29. Sarma, B.K.; Yadav, S.K.; Singh, S.; Singh, H.B. Microbial consortium-mediated plant defense against phytopathogens: Read-dressing for enhancing efficacy. *Soil Biol. Biochem.* **2015**, *87*, 25. [[CrossRef](#)]
30. Park, S.; Seo, Y.-S.; Hegeman, A.D. Plant metabolomics for plant chemical responses to belowground community change by climate change. *J. Plant Biol.* **2014**, *57*, 137. [[CrossRef](#)]
31. Munir, S.; Li, Y.; He, P.; He, P.; Ahmed, A.; Wu, Y.; He, Y. Unraveling the metabolite signature of citrus showing defense re-sponse towards Candidatus Liberibacter asiaticus after application of endophyte Bacillus subtilis L1-21. *Microbiol. Res.* **2020**, *234*, 126425. [[CrossRef](#)]
32. Schelli, K.; Zhong, F.; Zhu, J. Comparative metabolomics revealing Staphylococcus aureus metabolic response to different antibiotics. *Microb. Biotechnol.* **2017**, *10*, 1764. [[CrossRef](#)] [[PubMed](#)]

33. Moye, Z.D.; Zeng, L.; Burne, R.A. Fueling the caries process: Carbohydrate metabolism and gene regulation by *Streptococcus mutans*. *J. Oral Microbiol.* **2014**, *6*, 24878. [[CrossRef](#)]
34. Peng, B.; Su, Y.-B.; Li, H.; Han, Y.; Guo, C.; Tian, Y.-M.; Peng, X.-X. Exogenous Alanine and/or Glucose plus Kanamycin Kills Antibiotic-Resistant Bacteria. *Cell Metab.* **2015**, *21*, 249. [[CrossRef](#)]
35. Ren, W.X.; Han, J.; Uhm, S.; Jang, Y.J.; Kang, C.; Kim, J.-H.; Kim, J.S. Recent development of biotin conjugation in biological imaging, sensing, and target delivery. *Chem. Commun.* **2015**, *51*, 10403–10418. [[CrossRef](#)]
36. Zhang, A.; Ackley, B.D.; Yan, D. Vitamin B12 Regulates Glial Migration and Synapse Formation through Isoform-Specific Control of PTP-3/LAR PRTP Expression. *Cell Rep.* **2020**, *30*, 3981. [[CrossRef](#)] [[PubMed](#)]
37. Haruta, S.; Kato, S.; Yamamoto, K.; Igarashi, Y. Intertwined interspecies relationships: Approaches to untangle the microbial network. *Environ. Microbiol.* **2009**, *11*, 2963. [[CrossRef](#)]
38. Embree, M.; Liu, J.K.; Al-Bassam, M.M.; Zengler, K. Networks of energetic and metabolic interactions define dynamics in microbial communities. *Proc. Natl. Acad. Sci. USA* **2015**, *112*, 15450. [[CrossRef](#)]
39. Du, J.; Zhou, J.; Xue, J.; Song, H.; Yuan, Y. Metabolomic profiling elucidates community dynamics of the *Ketogulonigenium vulgare*–*Bacillus megaterium* consortium. *Metabolomics* **2012**, *8*, 960. [[CrossRef](#)]
40. Westhoff, S.; van Wezel, G.P.; E Rozen, D.E. Distance-dependent danger responses in bacteria. *Curr. Opin. Microbiol.* **2017**, *36*, 95. [[CrossRef](#)]
41. Mishra, J.; Arora, N.K. Secondary metabolites of fluorescent pseudomonads in biocontrol of phytopathogens for sustainable agriculture. *Appl. Soil Ecol.* **2018**, *125*, 35. [[CrossRef](#)]
42. Schulz-Bohm, K.; Zweers, H.; de Boer, W.; Garbeva, P. A fragrant neighborhood: Volatile mediated bacterial interactions in soil. *Front. Microbiol.* **2015**, *6*, 1212. [[CrossRef](#)]
43. Myo, E.M.; Liu, B.; Ma, J.; Shi, L.; Jiang, M.; Zhang, K.; Ge, B. Evaluation of *Bacillus velezensis* NKG-2 for bio-control activities against fungal diseases and potential plant growth promotion. *Biol. Control* **2019**, *134*, 23. [[CrossRef](#)]
44. Xu, L.; Ren, L.; Chen, K.; Liu, F.; Fang, X. Putative role of IAA during the early response of *Brassica napus* L. to *Plasmodiophora brassicae*. *Eur. J. Plant Pathol.* **2016**, *145*, 601–613. [[CrossRef](#)]
45. Lemarié, S.; Robert-Seilaniantz, A.; Lariagon, C.; Lemoine, J.; Marnet, N.; Jubault, M.; Manzanares-Dauleux, M.J.; Gravot, A. Both the Jasmonic Acid and the Salicylic Acid Pathways Contribute to Resistance to the Biotrophic Clubroot Agent *Plasmodiophora brassicae* in *Arabidopsis*. *Plant Cell Physiol.* **2015**, *56*, 2158–2168. [[CrossRef](#)] [[PubMed](#)]
46. Zhao, Y.; Qian, G.; Ye, Y.; Wright, S.; Chen, H.; Shen, Y.; Liu, F.; Du, L. Heterocyclic Aromatic N-Oxidation in the Biosynthesis of Phenazine Antibiotics from *Lysobacter antibioticus*. *Org. Lett.* **2016**, *18*, 2495–2498. [[CrossRef](#)]
47. Nawaz, N.U.A.; Saeed, M.; Khan, K.M.; Ali, I.; Bhatti, H.A.; Sabi-Ur-Rehman; Shahid, M.; Faizi, S. Isolation of tyrosine derived phenolics and their possible beneficial role in anti-inflammatory and antioxidant potential of *Tithonia tubaeformis*. *Nat. Prod. Res.* **2020**, *19*, 1–9. [[CrossRef](#)]